

<https://doi.org/10.33472/AFJBS.6.6.2024.157-173>



African Journal of Biological Sciences



Open Wound Treatment with Combination of Urinary Bladder Matrix (UBM), Nanosilver and Laser Therapy

Sameer Sabri Kadhim* and Abdulsatar Salman Hamza

Department of Surgery and Obstetric, College of Veterinary Medicine, University of Al-Qadisiyah, Iraq

*Email: vet21.post19@qu.edu.iq

Article History

Volume 6, Issue 6, Feb 2024

Received: 01 Mar 2024

Accepted: 08 Mar 2024

doi:10.33472/AFJBS.6.6.2024.157-173

Abstract

The purpose of this study was to investigate the effects of a combination of UBM, Nanosilver, and Laser on open wounds in rabbits. Thirty mature white rabbits from New Zealand weighing 1 ± 0.300 kg were studied, and all animals shared the same standards of bedding and ambient conditions. They were used and randomly separated into two groups ($n = 15$), ranging in age from 9 to 12 weeks. After general anesthesia and animal preparation for aseptic surgery, one open parallel circular full-thickness (1.5 cm in diameter) skin incision was produced on the back of the animals using a punch machine. The rabbits were sorted into two equal groups at random. histopathological specimens were collected at 7, 14, and 21 days after wounding. Skin wounds in Group (1) were left untreated as a control group. In Group (2), combination of lyophilized bovine UBM was used as scaffold in treatment of induced wound at first day after surgical operation, while the hydrogel of bovine UBM 2gm is used topically from second day after surgical operation until 7 days, once daily, nanosilver 0.5% ointment enough to cover the wound, and an 8 j/cm², 20 sec laser. The result showed the superiority of the combination of lyophilized bovine UBM, nanosilver and laser in wound healing.

Keywords: open, wound, combination, UBM, nanosilver, laser.

Introduction

Many researchers have tried materials that can assist enhance the environment of the wound bed in order to advance in the treatment of severe wounds and tissue restoration during the last few decades. Decellularized extracellular matrix (ECM) known as urinary bladder matrix (UBM) is applied in a variety of clinical cases. Clinical applications of the commercialized UBM include the therapy of diabetic ulcers, the reinforcement of gastrointestinal tissue, the reinforcement of urologic and gynecologic surgical procedures, the reinforcement of skin wounds, and the management of deep, partial thickness burns (Sadler, et al., 2017). ECM scaffold materials consist of the structural and functional components that make up the original tissue's ECM, including collagen, laminin, fibronectin, growth factors, glycosaminoglycans, glycoproteins, and proteoglycans (Costa, et al., 2017). silver has long been used in wound dressings to treat a variety of wounds, including burns, chronic ulcers, toxic epidermal necrolysis, and others (Mallakpour, et al., 2021). The antibacterial activity of nanosilver particles (AgNPs) against both Gram-positive and Gram-negative bacteria has been demonstrated. It has not yet been thoroughly investigated how exactly they exert their bactericidal or growth-inhibitory effects. The experimental data now available supports a number of theories that take into consideration AgNPs' physical properties, such as size and surface, which allow them to interact with or even pass through cell walls or membranes and directly change intracellular components (Cavassin, et al., 2015). Low level laser therapy (LLLT), which also had a favorable impact on collagen deposition in the wounds, sped up the epithelialization and inflammatory processes. In wounds that had been treated, the amount of collagen fibers increased, and the remodeling maturation phase was more obvious (Gal, et al., 2006). Collagen types I (80-85%) and III (10-15%) make up the dermal matrix in adult skin. Compared to the photothermal effect, the photomechanical effect substantially favors the production of collagen type III (Liu, et al., 2008). The aim of this research was to study Combination of UBM ,Nanosilver and Laser on Open Wounds in Rabbits.

Materials and methods :

Thirty mature white rabbits from New Zealand weighing 1 ± 0.300 kg were studied, and all animals shared the same standards of bedding and ambient conditions. They were used and randomly separated into two groups (n = 15), ranging in age from 9 to 12 weeks. One open parallel circular full-thickness (1.5 cm in diameter) skin incision was created on the back of the animals using a punch machine after general anesthesia and animal preparation for aseptic surgery. The rabbits were sorted into two equal groups at random. histopathological specimens were collected at (7, 14, and 21 days after wounding). During the conduct of the study, the national guidelines for the handling and use of laboratory animals were adhered to. Individually restrained, the animals were housed in stainless steel cages with a plastic cover in standard

laboratory settings (room temperature 20-24 °C and humidity 60%), where they also received anti-worm medication prior to the experiment. carrying out clinical and lab tests to make sure he is disease-free. The High Committee for Review and Approval of Research Proposals of the Faculty of the University of Al-Qadisiyah College of Veterinary Medicine gave its approval to all protocols.

Experimental Design:

Skin wounds in Group (1) were left untreated as a control group. In Group (2), combination of lyophilized bovine UBM was used as scaffold in treatment of induced wound at first day after surgical operation, while the hydrogel of bovine UBM 2gm is used topically from second day after surgical operation until 7 days, once daily, nanosilver 0.5% ointment enough to cover the wound, and an 8 j/cm², 20 sec laser.

Preparation of Decellularization Bovine Urinary Bladder Matrix: Fresh urinary bladders were harvested from recently slaughtered cows at the local slaughterhouse, and UBM-ECM was created as a decellularized scaffold in accordance with the instructions given by Rosario, *et al.* (2008). In order to make it easier to trim and remove fatty tissue and exterior connective tissues with scissors, the urinary bladder was briefly filled with tap water and then washed by it. With a knife scrape, the tunica serosa, tunica muscularis, and the majority of the muscularis mucosa were manually separated from the bladder tissue, resulting in a flat rectangular sheet. By submerging the sheet in a solution of 0.1% peracetic acid (PAA) and 4% ethanol solution on a shaker for two hours, the residual (sub-mucosal layer) was then decellularized and disinfected. The ECM was next rinsed in PBS (pH 7.4), 100 IU/ml penicillin, 100 g/ml streptomycin, and 100 g/ml amphotericin combined at 25 °C with trembling, in two changes of deionized water, and finally in one change of PBS, lasting 15 minutes each. The resulting decellularized ECM scaffolds were then stored at 4 °C for five hours before being terminally sterilized by immersion in PBS containing antibiotics and antifungal medications.

Preparation of Bovine Urinary Bladder Matrix Hydrogel: The urinary bladder submucosa hydrogels were obtained as previously described by (Freytes, *et al.*, 2008). The decellularized UBM sheets were moved to -20°C for 24 hours, then to a deep freezer at -80°C for 5 days. The scaffolds were then freeze dried in a freeze dryer (FTS Systems Bulk Freeze Dryer Model 8-54) for lyophilization until they were completely dry, chopped into small sheets for immersion in liquid nitrogen, and reduced to small pieces by a rotary knife mill. A sterile container was afterwards used to store the obtained powder after it had been sterilized at 60°C in a dry oven for 16 hours. The urinary bladder submucosa hydrogels were made quickly by digesting 100 mg of comminuted UBM in 10 mL of pepsin (Gibco USA), 3 mg/mL in 0.01 N hydrochloric acid (Gibco USA), for 48 hours at room temperature. The pH of the pre-gel samples was then neutralized to 7.4 using 0.1 N NaOH and PBS (10-1), which was done at 4 °C. Hydrogels were then created by incubating the samples at 37 °C for one hour.

Nanosilver ointment fabrication :Nanosilver (5gm) were purchased from local market and (0.5gm) of nanosilver mixed with (99.5 gm) Vaseline according to (Bold, *et al.*,2022).

Characterization of nanoparticles: Before using the materials in the experiment, the particle sizes of the materials utilized in this study, silver, were determined using UV, FTIR, and SEM. The data is stored in an electronic program. arranged for this purpose, which includes an average particle size image and a cure graph.

1. Ultraviolet visible analysis:By passing UV rays through a curette containing 1 cm of nanoscale solution and measuring the absorbance at various time intervals within the wavelength, a UV-visible spectrophotometer was used to calculate UV absorbance. The absorbance was registered within data that included a cure graph and a numerical table to calculate the wavelength recorded at the highest absorption rate, to determine the extent of change in material stability and dispersion before using it in the experiment.

2. Fourier Transform Infrared spectroscopy analysis: With the aid of an FTIR spectrometer (8400S, Shimadzu, Japan), Fourier Transform Infrared Spectroscopy analysis (FTIR) was carried out.

3. Scanning Electron Microscopy analysis: For the purpose of understanding the morphological and size characteristics of nanoparticles, including the form of the particles, their nanoscale size, the degree of isolation of the particles from one another, and general appearance, scanning electron microscopy analysis (SEM) was used.

Laser treatment: For laser treatment in G3 and G4, the Gallium Aluminum Arsenide Laser (GaALAs) (Omega Laser System Limited UK) , a diode laser with a wave length of 660 nm, power of 50 mw, and pulse rate of 146, was used. Its energy density was 8J/cm². After creating an open skin wound, laser treatment was applied immediately. For seven days straight, it was performed once daily at the same time. On the of the wounds, a laser probe was apparent, closed and perpendicular.

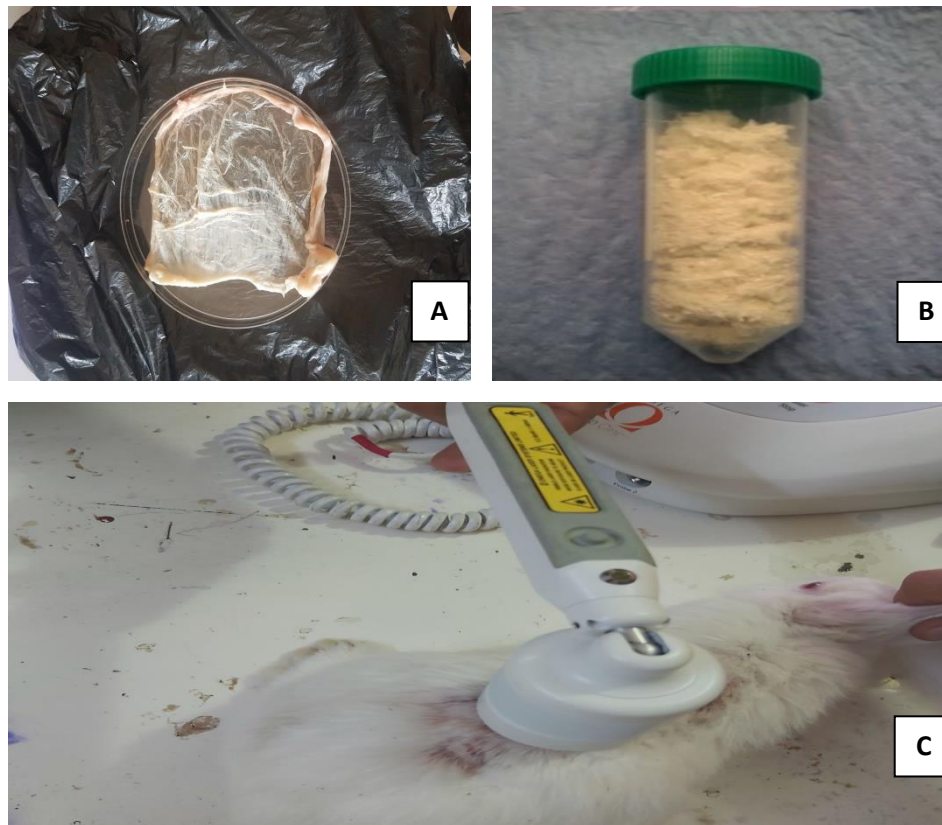


Fig.-1: Photograph showing the steps of bovine UBM-powder fabrication
 A. Mechanical separation of mucosal and seromuscular layers from the submucosa of bovine urinary bladder. B. Lyophilizing the urinary bladder UBM powder. C. laser treatment of the wound

Anesthesia of animals: To prevent the animals from pain or moving around during the circular skin incision, general anesthesia was employed together with the pre-medication anesthetic Diazepam 1mol/g IV. Utilizing an intramuscular injection of a combination of xylazine 2% (3 mg/kg B.w.) and ketamine (30 mg/kg B.w.) during the experiment (Abdullah, *et al.*, 2019).

Surgical Procedure :Following general anesthesia, the animal's back's incision site was prepared for aseptic surgery. These injured rabbits were distributed at random. Into four groups based on their chosen treatment approach. The backs of all of rabbit in all groups were inflicted with a 1.5 cm full thickness circular skin incision.(clipping, shaving, cleaning the region, applying povidine iodine as an antiseptic, and covering the area with gauze soaked in 70% alcohol) on the lateral thoracic side. By using a punch machine, a full-thickness skin incision measuring 1.5 cm in diameter was created. and left the control group untreated us group. Group(2) received treatment for the incision with lyophilized bovine UBM was use as scaffold in treatment of induce wound at first day after surgical operation , while the hydrogel of bovine UBM 2gm is use topically from second day after surgical operation until 7

days, once daily , nanosilver 0.5% ointment enough to cover the wound , and an 8 j/cm², 20 sec laser.

Preparation of specimens for histopathological examinations: Specimens of healed skin (wound biopsies) (2 cm³) were taken at (7,14, and 21) days post wounding (PW) from all animals after anesthesia of animals. The specimens were preserved in 10% neutral buffered formalin solution and send for histopathological examination after sectioning in 5 µm and staining with Hematoxylin and Eosin stain to evaluate the progress of healing process (S Kim, 2019 ; Estevao et., al. 2019).

Measurement of wound contraction: Wound contraction at 3th,7th , 14th and 21th days post wounding (PW) was calculated as percentage of the reduction in original wound area size by using the following formula: Percentage of wound contraction = (total wound size on (day/n) - wound area on day n / wound area on day 0 x 100) as % original wound (Sardari et. al., 2006; Patil et. al., 2012).

Statistical analysis: Morphometric data were statistically analyzed, using ANOVA test, and Least Significant Difference (LSD) to find the significance between groups under the level of P<0.05 (Weinberg and Abramowitz, 2008).

Results:

Characterization of nanoparticles

Uv-visible spectrophotometer analysis: UV–vis spectra was recorded, using an Agilent 8453 spectrophotometer with a 1 cm path length quartz cuvette. The UV-visible absorption spectra within the 200–1100 nm range of silver nanoparticles is shown in Fig.-2 The silver nanoparticles NPs exhibit absorption bands in the wavelength of 451 nm.

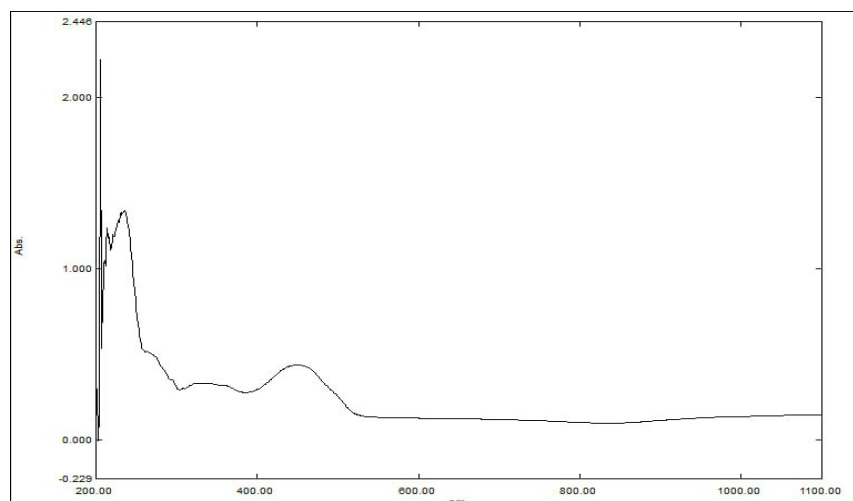


Fig. -2: UV–vis spectra of Ag nanoparticles

Scanning Electron Microscope analysis (SEM): The size and morphology of silver nanoparticles (AgNPs) was showed via scanning electron microscope. Analysis of SEM exhibited that Ag NPs were spherical in shape. A scan depiction of the AgNPs

was noted that its particle size of the Nano-metric scale was valued at 34.28 ± 0.81 nm at range of 22 to 46 as shown in (Fig-3).

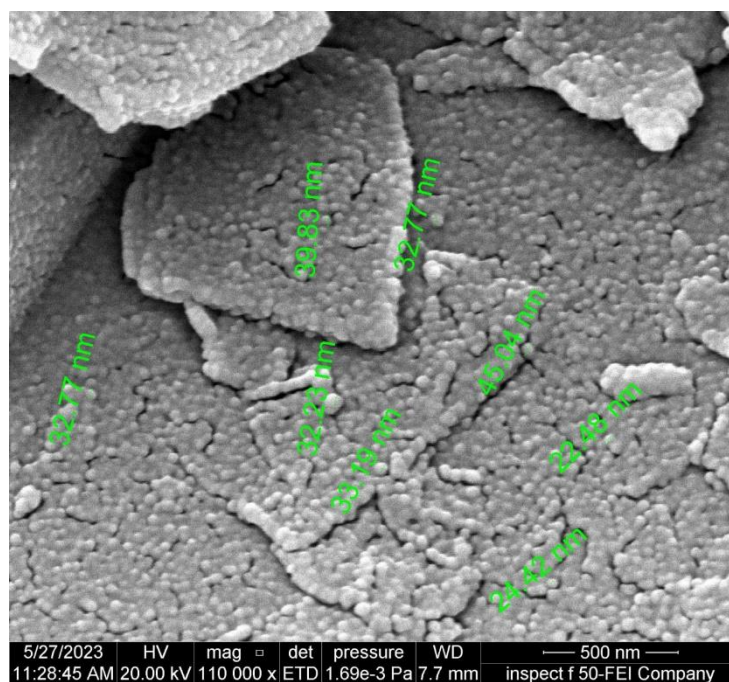


Fig. -3 SEM image (magnification 500 nm) of the Ag nanoparticles

FT-IR analysis: As shown in the Fig.- 4 the results exhibited that the spectra of FTIR of AgNps showed peaks at 3429.43; 2978.09; 2885.51; 1762.94, 1573.91, 1419.61, 1338.6; and 1014.56 cm^{-1} . The purified nanoparticles were observed in the presence of bands due to asymmetric stretching vibration of O–H bond (around 3429 cm^{-1}), also aldehydic C–H stretching (2978 cm^{-1}), C=O group (1762 cm^{-1}), C–C and C–N stretching (1338 cm^{-1}), and O–H stretch (1014.5 cm^{-1}). FTIR spectra determined data confirms the presence of O–H stretching (around 3429 cm^{-1}) which may be responsible for reducing metal ions into their respective nanoparticles.

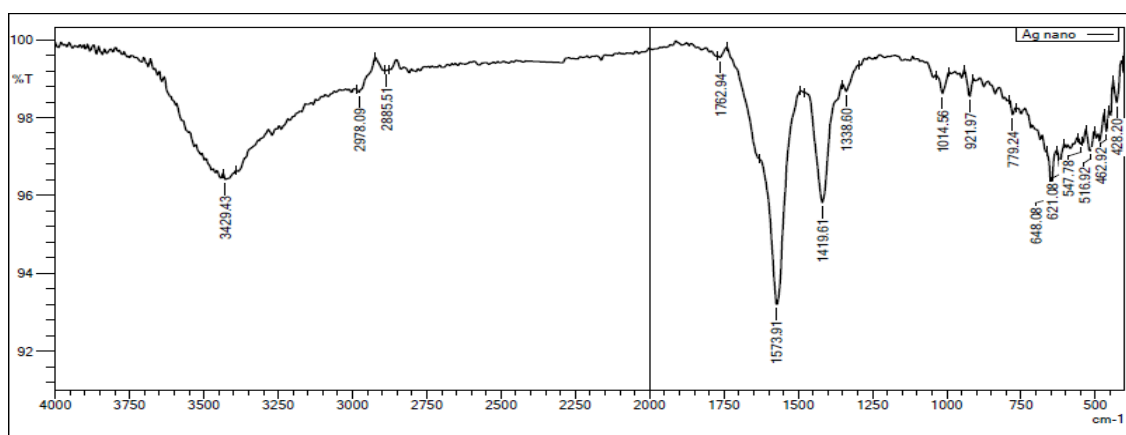


Fig. -4 FTIR spectra of the Ag nanoparticles

Morphometric assessment of the wound healing:

Clinical assessment : All animal groups were clinically viewed as being active, healthy, and having the usual healing mechanisms set up at the location of damage throughout the study 21 days post wounding (P.W). Whether the animals received treatment or not, there was no evidence of infection in any of their wounds, and no fatalities were noted. All wound locations began to swell and turn red within 4 hours of being injured, and they continued to do so while also growing larger over the course of the next 24 P.W. hours, with inflammatory signs intensifying. From the second day P.W. on, the entire wound enlarged, its boundaries were elevated and red in color, and the wound site developed a thick scab as a result of blood drying out, which continued into the seventh day P.W. The wound gradually shrank in size until, on the 21st day, it decreased to a small area of scar tissue with a round or liner shape.

wound contraction: Results from this study were varied. Table -1 displayed the mean \pm SE of the diameter values of the wound contraction over the period of the study's 3th day, 7th day, 14th day and 21thday.

On the 3th day of the study, the results showed a significant decrease ($p \leq 0.05$) in wound diameter in G2 11 compared with G1 13.90 at the same time. On the 7th day of the study, the results showed a significant decrease ($p \leq 0.05$) in wound diameter in G2 8 compared with G1 12 at the same time. At the 14th day , there are significant decrease ($p \leq 0.05$) in results of wound diameter in G2 2 compared with G1 10 at the same time. On the 21th day of the study, the results showed a significant decrease ($p \leq 0.05$) in wound diameter in G2 0.51 , compared with G1 4.93 at the same time.

Table.-1: mean \pm SE of the diameter values of the wound contraction recorded in experimental rabbits.

| Groups | Diameters of the wound (mm) | | | | |
|--------------|-----------------------------|---------------------|---------------------|----------------------|----------------------|
| | 0 day | 3 th day | 7 th day | 14 th day | 21 th day |
| G1 (n=15) | 15 \pm 0Aa | 13.90 \pm 0.21Ab | 12 \pm 0.18Ac | 10 \pm 0.29Ad | 4.93 \pm 0.19Ae |
| G2 (n=15) | 15 \pm 0Aa | 11 \pm 0.18Db | 8 \pm 0.16Dc | 2 \pm 0.15Dd | 0.51 \pm 0.02De |

* LSD $_{0.05} = 0.408$

Macroscopic appearance: Macroscopic appearance of wounds of all groups showed at 3th day, 7th day, 14th day and 21thday as shown in fig.-5. At 7th day the wounds of G1 were dryness and darkness and there were clear decrease in the diameters, while in G2 it was rough, light pale and decrease At 14th day there were growth of little proliferation tissue and the decrease of diameter was continued in G1, while the

wounds in G2 were complete filled with proliferation tissue. At 21th day scar tissue growth were clear in G1, but the wounds of G2 were healed and difficult distinguish from the neighbor skin.

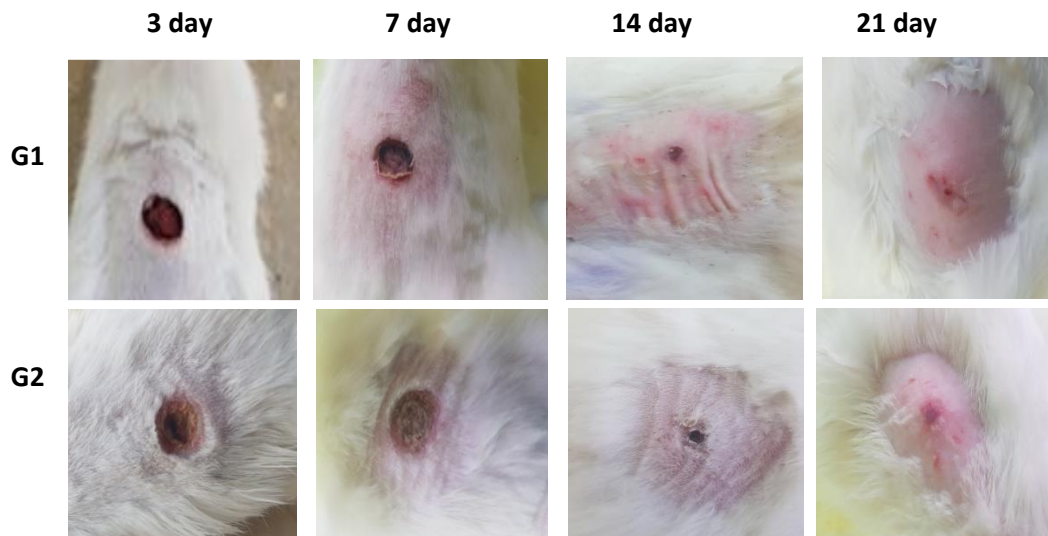
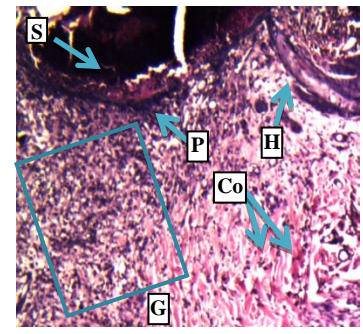
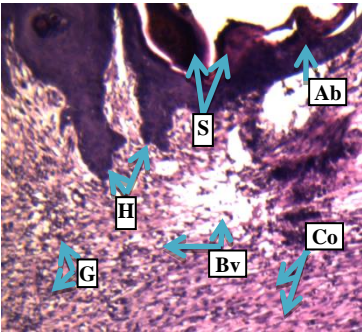
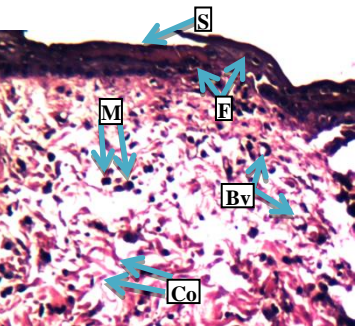
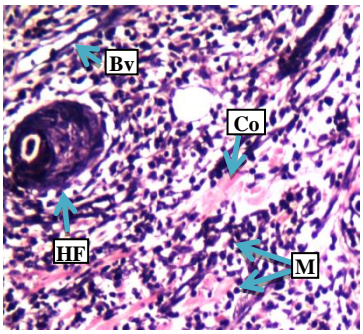
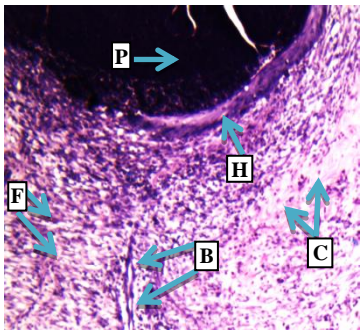
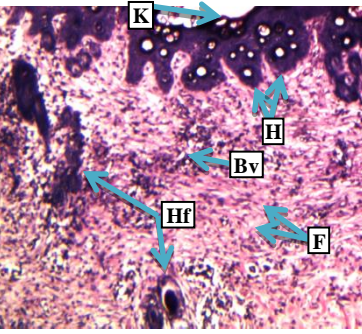


Fig -5: Morphological appearance of wounds of all groups at different periods.

Histopathological assessment of the wound healing: G1 at 7th a scab forms which covering over a site of healing. This scab appeared fractured and fragmented. Also there was pus present between the scab and the epidermis. There was mild hyperplasia of the epidermal layers. In the dermis, there was profuse granulation tissue (in which there was proliferation of the endothelial cells and fibroblasts). Also there was collagen in the site of injury as in Fig.-6. G2 at 7th showed new formation of hair follicle, infiltration of macrophages and lymphocytes, newly-formed blood vessels and fine network of collagen fibers in the dermis Fig. -7. G1 at 14th days showed formation of scab and abscess over the epidermis. Marked downward hyperplasia of stratum basale of the epidermis. Moderate granulation tissue with profuse collagen that replaces damaged tissue and formation of small new blood vessels in the dermis as in Fig. -8. G2 at 14th days showed an abscess formation over the epidermis. Marked hyperplasia of epidermal layers along the wound site. Newly-formed blood vessels vertically on the site of injury and marked fibrosis. Profuse collagen fibers which replace the site of wound as in Fig. -9. G1 at 21th days showed a small scab which showed over the site of injury. The tow edges of skin wound appear almost bound together due to the hyperplasia of epidermal layers. In the dermis, fine of collagen fibers replaces the damaged tissue with scattered inflammatory cells mainly macrophages, and formation of new vascularization as in Fig. -10. G2 at 21th days showed almost normal skin tissue, notice keratinized layer above the epidermis, with profuse hair follicles and marked, thick and hyperplasia of the epidermal layers. In the dermis newly-formed blood vessels and horizontal fibrosis on the site of wound with new formation of hair follicle as in Fig. -11.

| | 7th | 14th | 21th |
|----|--|--|--|
| G1 |  |  |  |
| | <p>Fig.-6 A scab forms which covering over a site of healing(S). This scab appeared fractured and fragmented. Also there was pus (P) present between the scab and the epidermis. There was mild hyperplasia of the epidermal layers(H). In the dermis, there was profuse granulation tissue (in which there was proliferation of the endothelial cells and fibroblasts). Also there is collagen in the site of injury(Co). 20 X H&E.</p> | <p>Fig.-8 Formation of scab (s) and abscess over the epidermis (Ab). Marked downward hyperplasia of stratum basale of the epidermis. Moderate granulation tissue (G) with profuse collagen (Co) that replaces damaged tissue and formation of small new blood vessels (Bv) in the dermis. 20X H&E.</p> | <p>Fig.-10 A small scab (S) which showed over the site of injury. The tow edges (E) of skin wound appear almost bound together due to mild hyperplasia of epidermal layers. In the dermis, fine of collagen fibers (Co) replaces the damaged tissue with scattered inflammatory cells mainly macrophages (M), and formation of new vascularization (Bv).50X H&E.</p> |
| G2 |  |  |  |
| | <p>Fig.-7 New formation of hair follicle (HF), infiltration of macrophages and lymphocytes (M), newly-formed blood vessels (Bv) and fine network of collagen fibers (Co) in the dermis.20X H&E.</p> | <p>Fig.-9 An abscess formation (P) over the epidermis. Marked hyperplasia (H) of epidermal layers along the wound site. Newly-formed blood vessels (Bv) vertically on the site of injury and marked fibrosis (F) . Profuse collagen fibers (Co) which replace the site of wound. 20 X H&E.</p> | <p>Fig.-11 Almost normal skin tissue, notice keratinized layer (K) above the epidermis, with profuse hair follicles (HF) and marked, thick and hyperplasia(H) of the epidermal layers. In the dermis newly-formed blood vessels (Bv) and horizontal fibrosis (F) on the site of wound with new formation of hair follicle (HF).20 X H&E.</p> |

Discussion: The objectives of this study were to assess the effect of combination of UBM ,nanosilver and laser on open wounds in rabbits. In this study, rabbits were used because they were small animals, widely bred, inexpensive compared to the cost of larger animals, and had short life cycles (gestation, lactation, and puberty). Rabbits were also very docile and non-aggressive, making them easy to handle and observed (Mapara, *et al.*2012). UBM-ECM: It was discovered that ECM components such collagen, glycosaminoglycans, vitronectin, and laminin were superior at acting as natural therapeutic agents (Costa,*et al.*2017). Cytokines, growth factors, and interactions with ECM elements, mediated by integrin, receptors, and sticky molecules, all influence how cells involved in the healing process function. While

neutrophil and macrophage proteases remove damaged matrix components helping in the remodeling of the original scar tissue, matrix metalloproteinases generated by endothelial cells and fibroblasts allow these cells to migrate (Reinke and Sorg, 2012). Also, in my opinion it covers the wound completely and prevented any invasion of micro-organisms. Silver nanoparticles' properties promoted wound adhesion and healing, decreased bacterial load at the site of the incision, increased collagen deposition there, and had no adverse effects on the body as a whole (Chowdhury, et al., 2014). When compared to the control group after 7, 14, and 21 days after treatment, all groups' surface area and wound contraction considerably decreased, which was consistent with (Chauhan, et al., 2018) who discovered that silver nanoscales demonstrated an effective healing mechanism for wounds with visible wound contraction. When comparing the treated animal's surface area to that of the control group over the course of 7, 14, and 21 days, the silver nanoparticles group found that there were substantial reductions and this applicable with (Amer, et al., 2018) They reported that the wound area, the time it takes for a wound to heal, and the healing rate are all significantly reduced by this nanoscale substance. Compared to control groups, the application of LLLT at a dose of 8 J/cm² accelerated up the healing of surgically induced full-thickness skin wounds in rabbits by reducing the inflammatory phase, increased blood flow to the area, increasing collagen synthesis, and increasing fibroblast activity. More than 8J/cm² of LLLT, applied both in vivo and in vitro, resulted in the inhibition of inflammatory processes. Since inflammation is essential for wound healing, this inhibition was thought to be one of the main reasons why healing delayed longer than expected. Because it stimulates the invasion of inflammatory cells and the release of cytokines, prostaglandins, and angiogenic factors. Therefore, reducing the inflammatory response could delay the healing of wounds (Agaiby, et al., 2000). It has been noted that the use of high doses did not improve fibroblast proliferation; it has been suggested that lower doses (4 to 8 J/cm²) may be more effective in causing an increase in myofibroblastic proliferation. Higher doses may cause additional stress on the cells and reduce migration and proliferation viability as well as mitochondrial activity (Medeiros, et al., 2010). This result is consistent with that of (Hussein, et al., 2019), who found that LLLT treatment using 660 nm resulted in a faster healing process when compared to the control group. This data supports the bio stimulatory effects of high-power pulsing light in the current study.

Macroscopic Findings: G1 at 7th PW displayed redness, and the wound's diameter was the same as when it was first created because fibroblast did not still grow. It's worthwhile to mention the results for G2 indicated that the synergistic combination of UBM, nano silver, and laser caused the wound to contract excessively or to shrink in size. Collagen and elastin production, revascularization, wound contraction, and collagen and elastin accumulation are only a few of the vascular and cellular changes that occur during wound healing. The trophic regeneration, anti-inflammatory information, and analgesic qualities are also noteworthy because they are all essential for completing the healing process. There are claims that this low-level laser therapy

increases mitochondrial activity, ATP, vasodilation, protein synthesis, the reduction of anti-inflammatory prostaglandins, cell mitosis, and the relocation and multiplication of keratinocytes. However, there are also claims that it encourages the growth of new capillaries, that its analgesic properties enhance the effect of UBM in protecting the wound from infection, and that it serves as a scaffold for fibroblasts. This promotes wound healing; several researches concur with these study's findings (Diller and Tabor, 2022 ; Brown, *et al.*2010). Silver nanoparticles block cells' respiratory pathways, keeping them alive to reproduce skin cells (fibroblast and keratinocytes), which could result in its reconstruction over time and eventual repair of the skin surface and Because of its safety, low cost, low toxicity, and broad-spectrum resistance to microbes, nanoscale silver plays an important role in the healing of wounds (Rigo, *et al.*,2013; Konop, *et al.*,2016). According to the findings of the current study, UBM, nanosilver, and laser have a synergistic impact whereby each one of them lessens the negative effects of the other. UBM and nanosilver lessen the toxicity of laser irradiation as well as its heat side effect on the skin (El-Gendy, *et al.*,2021). Light redness was present on G1 at 14th P.W, and the wound's diameter was less. G2 results at 14th P.W showed not much redness and that the wound was almost closed. Due to the synergistic effects of the three therapies, which had anti-microbial and anti-inflammatory effects as well as laser action on angiogenesis, smooth skin, removal of fibrous tissue, and increased absorption of UBM components and nanosilver, the healing of the lesion was almost complete. According to earlier studies, antioxidants are necessary for collagen synthesis, decreased inflammation, and angiogenesis these results agree with (Ambiga *et al.*, 2007). G1 at 21th P.W showed nearly reduction in diameter of the wound and scar tissue formation was visible clearly. These results were due to G1 left with no any treatment. G2 showed complete healing with no scar tissue due to the power synergistic effect of therapies on tissue healing, so it was the best in compare with other groups. The size, surface, and quantum tunneling properties of nano-structured silver make it significantly more effective at inhibiting bacterial growth than regular silver. The metal is efficient against gram-positive and gram-negative, aerobic and anaerobic bacteria, yeast, fungus, and viruses because it disrupts the microbial respiratory cytochromes, electron transport, and DNA replication, found that supplementing porcine small intestinal mucosa with nano-silver has a powerful antibacterial effect, effectively reducing surgical site infection, agree with (Zhou, *et al.*, 2011). When proper Photobiomodulation protocols are followed, LLLT has a positive impact on wound healing because it stimulates biological processes that lead to the induction of cytokines and the expression of growth factors by keratinocytes and stromal cells, which are key steps in the healing of soft tissue injuries (Hamblin and Demidova, 2006).

Microscopic Findings: G1 at 7th P.W a scab forms which covering over a site of healing. This scab appeared fractured and fragmented. Also there was pus present between the scab and the epidermis. There was mild hyperplasia of the epidermal layers agree with (Hussien, *et al.*, 2018 ; Albozachri, *et al.*, 2022). G2 showed

Marked downward hyperplasia of stratum basale. Profuse granulation tissue with irregular network of collagen fibers in the dermis, The epidermal layers showed thick and hyperplastic, infiltration of macrophages and newly-formed blood vessels. (You, et. al.,2017) they found Combining NAg with a dermal replacement could not only provide a carrier for particles to keep their in situ capabilities, but also give the scaffolds the potential to trigger an immune response and cell migration, resulting in a quick regeneration and high-quality repair. In order to effectuate the transformation of the dominant cell types, we conclude that NAg can control local inflammatory responses and enhance fibroblast migration via interacting with macrophages and fibroblasts. Light is used to stimulate fibroblast development, which leads to cellular multiplication, increasing collagen synthesis. Better energy absorption by the mitochondria may have increased ATP and DNA synthesis, which in turn improved collagen synthesis, epithelial repair, and granulation tissue growth (Giuliani, et al., 2009). According to the study's findings, the combination of UBM, nanosilver, and laser in G2 produced the greatest and most effective wound healing results. In the current study the G1 at 14th P.W showed the presence of moderate granulation tissue caused the rate of re-epithelialization to slow down, which in turn caused the wound size to not contract clearly .These findings were in accordance with (Armstrong and Meyr, 2022). In G2 the result showed an abscess formation over the epidermis. Marked hyperplasia of epidermal layers along the wound site. Newly-formed blood vessels vertically on the site of injury and marked fibrosis. Profuse collagen fibers which replace the site of wound and also there is infiltration of inflammatory cells with new formation of hair follicle which contain hair. These results correlated (Hussein, et al., 2011) who reported that employing low-level laser therapy (LLLT) for wound treatment led to faster wound healing, which can be attributed to increased collagen production by fibroblasts, significant vascular proliferation in connective tissue, and increased cell mitosis. These findings are in accordance with earlier studies by (Amer, et al., 2018; Chowdhury et al., 2014)who reported that silver nano particles were not only effective as antimicrobial agents but also improved the quality of healed cutaneous wounds, which were evidently observed histopathologically. Silver nano particles also showed positive influences on skin wound healing through reducing inflammation, preventing infection, and promoting tissue vasculature. According to (Kandaswamy, et al.,2013) who described the mechanism of action of UBM in promoting wound healing, the beneficial effects of these bioimplants could be obtained either directly by ECM molecules or indirectly by their bioactive signal molecules within the UBM; such as growth factors, cytokines, chemokines, and hormones. A small scab which showed over the site of injury in G1 at 21th days . The tow edges of skin wound appear almost bound together due to the hyperplasia of epidermal layers. In the dermis, fine of collagen fibers replaces the damaged tissue with scattered inflammatory cells mainly macrophages, and formation of new vascularization , results accompanied with (Miller and Zachary,2017) . New vascularization in which new blood vessels are formed, fibroblast proliferation which produce the collagen that replaces the site of injury. macrophage infiltration (Schultz,et al.,2011). In G2 showed almost normal skin tissue, notice keratinized layer

above the epidermis, with profuse hair follicles and marked, thick and hyperplasia of the epidermal layers. In the dermis newly-formed blood vessels and horizontal fibrosis on the site of wound with new formation of hair follicle because of the power effect of all therapies antibacterial, anti-inflammatory, acceleration of proliferation of fibroblasts, stimuli macrophages and angiogenesis process that included in the study as mention by (Huimin, et al.2023; Diller and Tabor,2022 ; Ragab, et al.,2021; Ghaemi, et al.,2019).

Conclusion: The treatments of open skin wounds with lyophilized bovine UBM improve the wound healing.

References:

- Abdullah BJ**, Atasoy N, Omer AK (2019). Evaluate the effects of platelet rich plasma (PRP) and zinc oxide ointment on skin wound healing. *Annals of Medicine and Surgery*.37: 30-37.
- Agaiyby**, A. D., Ghali, L. R., Wilson, R., & Dyson, M. (2000). Laser modulation of angiogenic factor production by T-lymphocytes. *Lasers in Surgery and Medicine: The Official Journal of the American Society for Laser Medicine and Surgery*, 26(4), 357-363.
- Albozachri**, J. M. K., Al-Arubaye, N., & Khudaier, A. M. (2022). histological study of skin wounds healing by use ethanol extract iraqi propolis dressing in rabbits. *biochemical & cellular archives*, 22(1).
- Ambiga** ,Agnelo Nerves Ms: Fernandes, Kristianne Porta (2007) Effect of low level laser therapy on healing.
- Amer SA**, Nouh SR, Elkammar MH, Shalaby TI, Korittum AS (2018).Silver Nanoparticles Preparation and their Effect on Full-thickness Skin Wound Healing in Rabbit Model.*Alexandria Journal for Veterinary Sciences*,57(2).
- Armstrong**, D., & Meyr, A. (2022). Basic principles of wound healing. Uptodate.[Internet]. Waltham (MA). UpToDate Inc.
- Bold**, B. E., Urnukhsaikh, E., & Mishig-Ochir, T. (2022). Biosynthesis of silver nanoparticles with antibacterial, antioxidant, anti-inflammatory properties and their burn wound healing efficacy. *Frontiers in Chemistry*, 10.
- Brown**, B. N., Barnes, C. A., Kasick, R. T., Michel, R., Gilbert, T. W., Beer-Stolz, D., ... & Badylak, S. F. (2010). Surface characterization of extracellular matrix scaffolds. *Biomaterials*, 31(3), 428-437.
- Cavassin**, E. D., de Figueiredo, L. F. P., Otoch, J. P., Seckler, M. M., de Oliveira, R. A., Franco, F. F., ... & Costa, S. F. (2015). Comparison of methods to detect the in vitro activity of silver nanoparticles (AgNP) against multidrug resistant bacteria. *Journal of nanobiotechnology*, 13(1), 1-16.
- Chauhan**, P. S., Shrivastava, V. I. K. A. S., Gbks, P. R. A. S. A. D., & Tomar, R. S. (2018). Effect of silver nanoparticle-mediated wound therapy on biochemical, hematological, and histological parameters. *Asian J. Pharm. Clin. Res*, 11, 251-258.
- Chowdhury S**, De M, Guha R, Batabyal S, Samanta I, Hazra SK, Hazra S (2014). Influence of silver nanoparticles on post-surgical wound healing following topical application.*European journal of Nanomedicine*.6(4): 237-247

Costa, A., Naranjo, J. D., Londono, R., & Badylak, S. F. (2017). Biologic scaffolds. Cold Spring Harbor perspectives in medicine, 7(9), a025676.

Diller, R. B., & Tabor, A. J. (2022). The role of the extracellular matrix (ECM) in wound healing: A review. Biomimetics, 7(3), 87.

El-Gendy, A. O., Samir, A., Ahmed, E., Enwemeka, C. S., & Mohamed, T.(2021). The antimicrobial effect of 400 nm femtosecond laser and silver nanoparticles on gram-positive and gram-negative bacteria. Journal of Photochemistry and Photobiology B: Biology, 223, 112300.

Estevao, L. D, Vieira, P., Leite, A. G. B., Bulhoes, A. V., Barcelos, L. S., and Neto, J. (2019). Morphological Evaluation of Wound Healing Events in the Excisional Wound Healing Model in Rats, Bio-protocol 9 (13): e3285.

Freytes, D. O., Martin, J., Velankar, S. S., Lee, A. S., & Badylak, S. F. (2008). Preparation and rheological characterization of a gel form of the porcine urinary bladder matrix. Biomaterials, 29(11), 1630-1637.

Gal, P. ; Vidinsky, B. ; TopoRcer, T. ; Mokry, M. ; Mozes, S. ; Longauer, F. and Sabo, J. (2006) . Histological assessment of effect of laser irradiation on skin wound healing in rats . Photomed Laser Surg. 24 : 480 – 488 .

Ghaemi, M., Sharifi, D., Mokmeli, S., Kowsari, G., Mortazavi, P., & Golmai, P. (2019). Comparison and evaluation of the low-level laser and the red and blue LED effects on wound healing in rabbit. Journal of Lasers in Medical Sciences, 10(3), 189.

Giuliani, A., Lorenzini, L., Gallamini, M., Massella, A., Giardino, L., & Calzà, L. (2009). Low infrared laser light irradiation on cultured neural cells: effects on mitochondria and cell viability after oxidative stress. BMC complementary and alternative medicine, 9, 1-10.

Hamblin, M.R. and T.N. Demidova(2006).. Mechanisms of low level light therapy. In Biomedical Optics International Society for Optics and Photonics.

Hussein, A. J., Alfars, A. A., Falih, M. A., & Hassan, A. N. A. (2011). Effects of a low level laser on the acceleration of wound healing in rabbits. North American journal of medical sciences, 3(4), 193.

Hussein, A. A., Munahi, A. K., & Alzamili, S. K. N. (2019) Low-Level Laser Therapy (Two Different Wavelengths 660nm and 820nm) Compared with Nigella Sativa Oil for Treatment of Burns in Rats.

Hussien, A. A., Munahi, A. K., & Farman, R. H. (2018). A comparison between Aloe vera and silver sulfadiazine on second-degree burns in local male rabbits: A Histological study. Al-Qadisiyah Journal of Veterinary Medicine Sciences, 17(1), 23-28.

Kandaswamy, K. K., Pugalenthi, G., Kalies, K. U., Hartmann, E., & Martinetz, T. (2013). EcmPred: prediction of extracellular matrix proteins based on random forest with maximum relevance minimum redundancy feature selection. Journal of theoretical biology, 317, 377-383.

- Konop**, Marek, Tatsiana Damps, Aleksandra Misicka, and Lidia Rudnicka. 2016. "Certain Aspects of Silver and Silver Nanoparticles in Wound Care: A Minireview." *Journal of Nanomaterials* 2016.
- Liu**, H. ; Dang, Y. ; Wang, Z. ;Chai, X. and Ren, Q. (2008) . Laser induced collagen remodeling a comparative study in vivo on mouse model . *J. of Laser in Surg. and Med.* 40 : 13 – 19.
- Mallakpour**, S., Hussain, C. M., Gulati, S., Kumar, S., Diwan, A., Singh,P., & Mongia, A. (2021). "Nanosilver": A Versatile and New-Generation Nanoproduct in Biomedical Applications. *Handbook of Consumer Nanoproducts*, 1-20.
- Mapara**, M., Thomas, B. S., & Bhat, K. M. (2012). Rabbit as an animal model for experimental research. *Dental research journal*, 9(1), 111.
- Mederios**, J. L. ; Nicolau, R. A. ; Nicola, E. M. ; dos Santos, J. N. and Pinheiro, A. L. (2010) . Healing of surgical wounds made with a 970 nm Diode laser associated or not with laser phototherapy . *J. of Photomed. and Laser Surg.* 28 : 489 – 496 .
- Miller**, M. A., & Zachary, J. F. (2017). Mechanisms and morphology of cellular injury, adaptation, and death. *Pathologic basis of veterinary disease*, 2.
- Patil M.V.K.**, Kandhare A.D., and Bhise S.D. (2012) Pharmacological evaluation of ethanolic extract of *Daucus carota* Linn root formulated cream on wound healing using excision and incision wound model; *Asian Pacific Journal of Tropical Biomedicine* (2012)S646-S655.
- Ragab**, G. H., Zaki, F. M., Hassan, F. E., & Safwat, N. M. (2021). Comparable Study of Different Materials (Silver Nanoparticles, PRP and its Mixture) That Enhance Surgical Excisional Skin Wound Healing in New Zealand Rabbits; Histopathological Evaluation. *Annals of the Romanian Society for Cell Biology*, 25(6), 15966-15975.
- Reinke**, J. M., & Sorg, H. (2012). Wound repair and regeneration. *European surgical research*, 49(1), 35-43.
- Rigo**, Chiara et al. 2013. "Active Silver Nanoparticles for Wound Healing." *International journal of molecular sciences* 14(3): 4817–40.
- Rosario**, D. J., Reilly, G. C., Ali Salah, E., Glover, M., Bullock, A. J., & MacNeil, S. (2008). Decellularization and sterilization of porcine urinary bladder matrix for tissue engineering in the lower urinary tract.
- S Kim**, S. (2019). *Bancroft's Theory and Practice of histological techniques eighth edition*/S. Kim Suvarna.
- Sadtler**, K., Sommerfeld, S. D., Wolf, M. T., Wang, X., Majumdar, S., Chung, L., ... & Elisseff, J. H. (2017, February). Proteomic composition and immunomodulatory properties of urinary bladder matrix scaffolds in homeostasis and injury. In *Seminars in immunology* (Vol. 29, pp. 14-23). Academic Press.
- Sardari K.**, Dehgan M. M., Mohri M., Emami M.R., Mirshahi A., Maleki M., Najar Barjasteh M., and Aslani M.R. (2006) Macroscopic aspects of wound healing (contraction and epithelialization) after topical administration of allicin in dogs; *Comp Clin Pathol*, 15:231–235.
- Schultz**, G. S., Chin, G. A., Moldawer, L., & Diegelmann, R. F. (2011). 23 principles of wound healing. *Mechanisms of vascular disease: a reference book for vascular specialists*, 423.

Wang, L., Johnson, J. A., Chang, D. W., & Zhang, Q. (2013). Decellularized musculofascial extracellular matrix for tissue engineering. *Biomaterials*, 34(11), 2641-2654.

You, C., Li, Q., Wang, X., Wu, P., Ho, J. K., Jin, R., ... & Han, C. (2017). Silver nanoparticle loaded collagen/chitosan scaffolds promote wound healing via regulating fibroblast migration and macrophage activation. *Scientific reports*, 7(1), 10489.

Zhang, Q., Li, N., Goebel, J., Lu, Z., & Yin, Y. (2011). A systematic study of the synthesis of silver nanoplates: is citrate a “magic” reagent?. *Journal of the American Chemical Society*, 133(46), 18931-18939.